Geometric Corner Extraction in Retinal Fundus Images*

Jimmy Addison Lee[1], Beng Hai Lee[1], Guozhen Xu[1], Ee Ping Ong[1], Damon Wing Kee Wong[1], Jiang Liu[1] and Tock Han Lim[2]

Abstract— **This paper presents a novel approach of finding corner features between retinal fundus images. Such images are relatively textureless and comprising uneven shades which render state-of-the-art approaches e.g., SIFT to be ineffective. Many of the detected features have low repeatability ($< 10\%$), especially when the viewing angle difference in the corresponding images is large. Our approach is based on the finding of blood vessels using a robust line fitting algorithm, and locating corner features based on the bends and intersections between the blood vessels. These corner features have proven to be superior to the state-of-the-art feature extraction methods (i.e. SIFT, SURF, Harris, Good Features To Track (GFTT) and FAST) with regard to repeatability and stability in our experiment. Overall in average, the approach has close to 10% more repeatable detected features than the second best in two corresponding retinal images in the experiment.**

I. INTRODUCTION

Ocular fundus images can provide information about retinal, ophthalmic, and even systemic diseases such as diabetes, hypertension, macular degeneration, and arteriosclerosis. These images, taken at different times or different fields of view, are sometimes spatially aligned for clinical review of disease progression or as a spatial map for laser guidance system during laser treatment. Computer vision methods for mosaicing retinal images would be a useful tool to achieve these goals. One of the most crucial tasks for image mosaicing is the identification of a possibly high number of interest points in all images of similar scene. “Interest point”, “corner”, “keypoint”, “salient point”, and “feature point” are used somewhat interchangeably. State-of-the-art interest point detection/description schemes, such as SIFT [10], have brought about important progress in image mosaicing [3], [4]. Yet, these methods have shown to fail in identifying sufficient number of salient points for building precise retinal image mosaics [5]. Many of these methods are designed for images with rich texture, such as images of outdoor scene. They do not work well on images which are relatively textureless such as retinal images.

In this paper, we evaluate some of the state-of-the-art feature extraction methods applied to retinal fundus images. On the other hand, we propose a technique to identify good corner features in retinal images which are generally superior to the state-of-the-art methods with regard to repeatability and stability. We detect blood vessels and form corners among them. These corners are true corners which each is formed by the intersection of two or more vessels, or a significant bend on a vessel. In contrast, computer vision’s corner detectors, e.g. Harris corner detector [8], are mainly based on the intensity change. A significant large amount of noise would be expected due to the uneven shades on the eye fundus. In the following, we will briefly introduce some of the related work regarding existing state-of-the-art feature extraction methods and then propose our feature extraction framework.

II. RELATED WORK

Existing retina mosaicing algorithms are mainly using area-based or feature-based approaches [2], [9], [12]. Feature-based approaches are more robust to illumination changes and significant initial-misalignment, and are therefore more appropriate for retina mosaicing. However, extracting of features in retinal images is difficult [5], [6]. Many of the retinal images are of poor quality whereby the so called salient points or corners are not easily detected. Scale Invariant Feature Transform (SIFT) [10], an algorithm for extracting distinctive invariant features, is one of the most popular feature-based approaches. The SIFT features are invariant to image scale and rotation. These features are highly distinctive in a sense that a single feature can be correctly matched with high probability against a large set of features from many images. However, the approach fails to identify sufficient number of good features when come to retinal fundus images [5]. Soon after, another simplified version of SIFT, named Speeded Up Robust Features (SURF) [1], was proposed. It is several times faster and more robust against different image transformations than SIFT claimed by its authors. SURF uses Hessian-matrix based detector to identify blob-like interest points which are claimed to be superior than other state-of-the-art feature extraction methods with regard to repeatability and stability. However, similar to SIFT, our experiments show that the number of good interest points detected very much depend on the quality of the retinal images.

A simple concept of finding interest points was proposed by Harris and Stephens [8] called Harris corner detector, which finds variation in intensity in all directions. It is probably the most widely used corner detector in the vision literature. However as mentioned earlier, the corners on the retinal images are either not very prominent, or are formed by some uneven shades (noise). Later in 1994, Shi and

*This work is supported by National Healthcare Group, Eye Institute, Tan Tock Seng Hospital, Singapore.

[1]J. A. Lee, [1]B. H. Lee, [1]G. Xu, [1]E. P. Ong, [1]D. W. K. Wong and J. Liu are with the Institute for Infocomm Research, Agency for Science, Technology and Research (A*STAR), Singapore {jalee, benghai, xug, epong, wkwong, jliu} at i2r.a-star.edu.sg

[2]T. H. Lim is with the National Healthcare Group (NHG), Eye Institute, Singapore tock_han_lim at nhg.com.sg

Tomasi [14] made a small modification to Harris corner detector, and introduced the Good Features to Track which finds corners based on quality. A more recent corner detector is the Features from Accelerated Segment Test (FAST) detector [15], which is derived from machine learning. The detector is claimed to having a high level of repeatability under large aspect changes and is much faster than other existing corner detectors such as Harris. However, the detector is not robust to high level noise.

In Section IV, we evaluate all the above mentioned detectors (SIFT, SURF (Hessian-matrix), Harris, Good Features to Track, and FAST) together with our proposed detector on the retinal fundus images.

III. Geometric corner detector

Our approach is based on the observation that corresponding blood vessels are more repetitively being detected even for images taken at different clinical visits. We find blood vessels by detecting edges which can be effectively characterized by line segments [13]. We extract line segments from an edge image by a strip fitting algorithm [11]. Due to the well-known fragmentation of edge maps of real images, missing edge pixels will result in the fracturing of a line segment. To circumvent this problem, a post-processing step is applied to identify and fix broken line segments. Let $L = \{\ell_1, \cdots, \ell_n\}$ represents a set of line segments found from [11]. Two line segments ℓ_i and ℓ_j are joined if the following condition is satisfied,

$$\begin{aligned} &Cond_{join}(\ell_i, \ell_j): \\ &\theta > \tau_\theta \;\; and \;\; \min\left(\|P_{k,i}, P_{k,j}\|_2\right) < \tau_d, \forall k \in \{1,2\}, \end{aligned} \tag{1}$$

where θ is the smaller internal angle between ℓ_i and ℓ_j, and τ_θ denotes the allowed internal angle threshold between ℓ_i and ℓ_j. $P_{k,i}$ indicates the k^{th} end point of ℓ_i, and τ_d denotes the allowed distance threshold between the shortest end-to-end point of ℓ_i and ℓ_j. We denote $\ell_{i,j}$ as the line segment formed by joining ℓ_i with ℓ_j. However, line segments that are relatively short (e.g., < 5 pixels) in $\hat{L}$ are removed as they are mainly insignificant lines or noise which are not blood vessels through our observation. A sample result is shown in Fig. 1(b).

Among these line segments, we find all intersections each between two or more line segments. We called them "geometric corners". Geometric corners are different from appearance-based corners such as Harris corners [8] as geometric corners are always real corners where each corner comes from an intersection of two or more line segments. Given two line segments ℓ_i and ℓ_j as first and second line segments with their end-to-end points as P_1P_2 and P_3P_4 respectively, $P_1 = (x_1, y_1)$, $P_2 = (x_2, y_2)$, $P_3 = (x_3, y_3)$, and $P_4 = (x_4, y_4)$, the intersection point $(x_{i,j}, y_{i,j})$ between ℓ_i and ℓ_j in parametric form is defined as

$$x_{i,j} = x_1 + t_i(x_2 - x_1), \tag{2}$$

$$y_{i,j} = y_1 + t_i(y_2 - y_1). \tag{3}$$

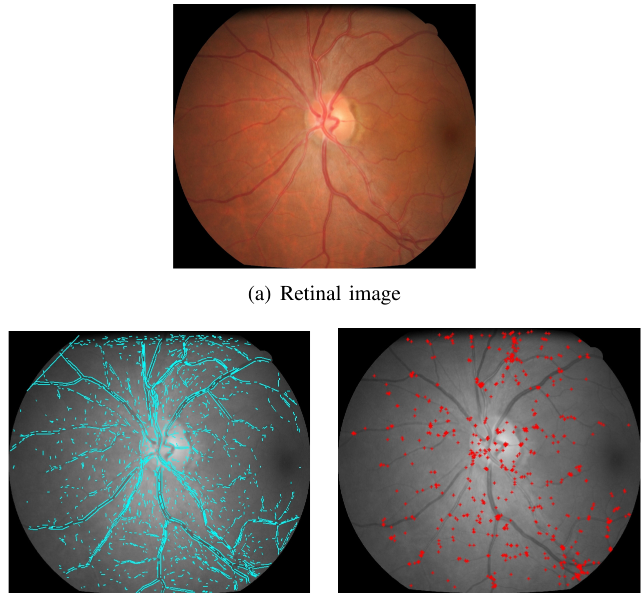

(a) Retinal image

(b) Line segment extraction

(c) Geometric corner detection

Fig. 1. Geometric corner detection process. (a) Original retinal image. (b) 1960 line segments extracted. (c) 771 geometric corners detected.

Solving for t_i yields

$$t_i = \frac{(x_4 - x_3)(y_1 - y_3) - (y_4 - y_3)(x_1 - x_3)}{(y_4 - y_3)(x_2 - x_1) - (x_4 - x_3)(y_2 - y_1)}. \tag{4}$$

If the denominator is not 0, then ℓ_i and ℓ_j are not parallel and are therefore either intersected or intersecting. We define a geometric corner as

$$\min\left(\|(x_{i,j}, y_{i,j}), P_{k,i}\|_2\right) < \tau_d, \tag{5}$$

$$and \;\; \min\left(\|(x_{i,j}, y_{i,j}), P_{k,j}\|_2\right) < \tau_d, \forall k \in \{1,2\}, \tag{6}$$

where τ_d denotes the allowed small distance threshold between the intersection point $(x_{i,j},\, y_{i,j})$ and the two closest end points from ℓ_i and ℓ_j. This approach is not exhaustive since not every two line segments can intersect within τ_d. A sample result is shown in Fig. 1(c). We can see that many good corner features are detected on the bends and between the intersections of the blood vessels all around the image.

IV. Evaluation

We evaluate the feature detectors discussed in Section II together with our geometric corner detection approach discussed in Section III on retinal fundus images. The six approaches are as follows:

- SIFT feature detector
- SURF feature detector
- Harris corner detector
- Good Features To Track (GFTT) detector
- FAST corner detector
- Geometric corner detector

The detection image results are displayed in Fig. 2. Many of these algorithms have at least a threshold that does not have a one-size-fits-all setting, it varies from image to image. We use four different threshold settings for every approach.

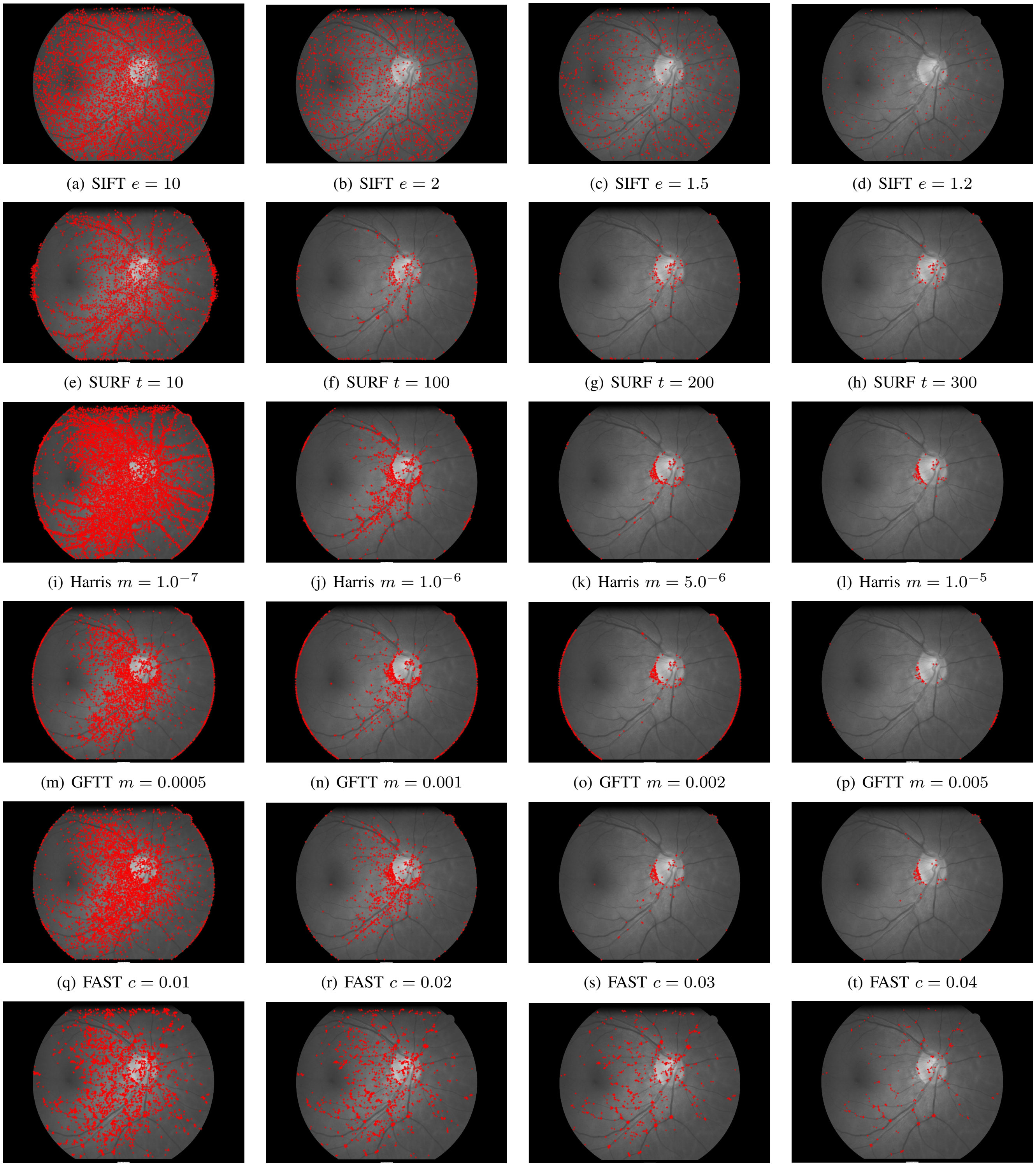

(a) SIFT $e = 10$ (b) SIFT $e = 2$ (c) SIFT $e = 1.5$ (d) SIFT $e = 1.2$

(e) SURF $t = 10$ (f) SURF $t = 100$ (g) SURF $t = 200$ (h) SURF $t = 300$

(i) Harris $m = 1.0^{-7}$ (j) Harris $m = 1.0^{-6}$ (k) Harris $m = 5.0^{-6}$ (l) Harris $m = 1.0^{-5}$

(m) GFTT $m = 0.0005$ (n) GFTT $m = 0.001$ (o) GFTT $m = 0.002$ (p) GFTT $m = 0.005$

(q) FAST $c = 0.01$ (r) FAST $c = 0.02$ (s) FAST $c = 0.03$ (t) FAST $c = 0.04$

(u) Geometric corners $l = 6$ (v) Geometric corners $l = 8$ (w) Geometric corners $l = 10$ (x) Geometric corners $l = 15$

Fig. 2. Six feature detection algorithms using different threshold settings. 1st column (a-d): SIFT feature detection with edge thresholds $e = 10, 2, 1.5, 1.2$ and nos. of detected features $= 6100, 2019, 840, 208$ respectively. 2nd column (e-h): SURF feature detection with metric thresholds $t = 10, 100, 200, 300$ and nos. of detected features $= 2971, 300, 134, 69$ respectively. 3rd column (i-l): Harris corner detection with min. quality thresholds $m = 1.0^{-7}, 1.0^{-6}, 5.0^{-6}, 1.0^{-5}$ and nos. of detected corners $= 8379, 998, 187, 83$ respectively. 4th column (m-p): Good Features To Track (GFTT) detection with min. quality thresholds $m = 0.0005, 0.001, 0.002, 0.005$ and nos. of detected corners $= 3043, 860, 447, 88$ respectively. 5th column (q-t): FAST corner detection with min. contrast thresholds $c = 0.01, 0.02, 0.03, 0.04$ and nos. of detected corners $= 4638, 855, 139, 69$ respectively. 6th column (u-x): Geometric corner detection with min. length of line thresholds $l = 6, 8, 10, 15$ and nos. of detected corners $= 3907, 1618, 811, 327$ respectively.

From the figure, we can visually see that SIFT and our geometric corner approaches produce the most well-scattered feature points around the retinal surfaces. However for SIFT features, most of the features are detected on the uneven shades on the retinal surfaces, these shades are not repetitive on other corresponding retinal images of different views or taken at different periods of time as illustrated in Fig. 3. In contrast, geometric corner approach produces many more repeated corner features on the bends and intersections between the vessels. Figure 3 displays the feature detection results of the six algorithms on a corresponding image of Fig. 2 taken in a different viewing angle. We deliberately choose image pairs with viewing angle differences which are rather large. We determine some repeated feature points in each pair of corresponding images and use RANSAC [7] to evaluate the rest of the repeated points. In term of repeatability scores, SIFT achieved 4.7%, SURF achieved 7.3%, Harris achieved 4.5%, GFTT achieved 5.7%, FAST achieved 5.5%, and geometric corners achieved 17.6%. The results clearly reveal that geometric corner approach significantly outperforms the other five approaches in term of repeatability. We evaluate another 19 more pairs of retinal images and results are rather consistent. Overall in average, geometric corner approach has achieved 9.6% more repeated feature points than SURF, SURF has achieved 1.4% more than SIFT, SIFT has achieved 0.8% more than GFTT, GFTT has achieved 0.2% more than FAST, and lastly FAST has achieved 0.6% more than Harris.

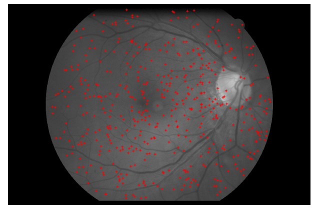

(a) SIFT $e = 1.5$

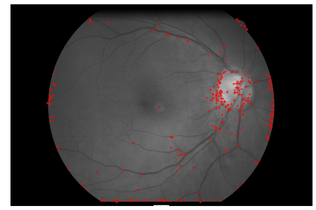

(b) SURF $t = 100$

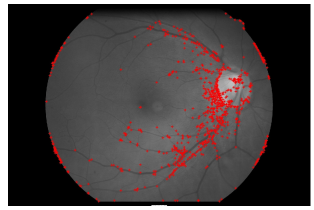

(c) Harris $m = 1.0^{-6}$

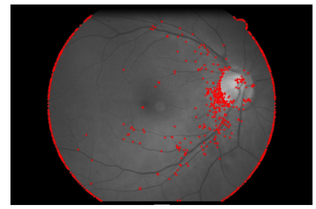

(d) GFTT $m = 0.001$

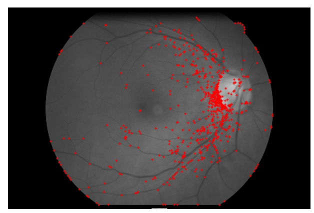

(e) FAST $c = 0.02$

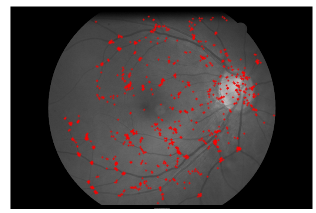

(f) Geometric corners $l = 10$

Fig. 3. Feature detection by the six approaches on the corresponding retinal image of Fig. 2 in a different viewing angle. SIFT detected 555 features, 4.7% repeated from Fig. 2. SURF detected 780 features, 7.3% repeated from Fig. 2. Harris detected 833 features, 4.5% repeated from Fig. 2. GFTT detected 736 features, 5.7% repeated from Fig. 2. FAST detected 684 features, 5.5% repeated from Fig. 2. Geometric corners detected 1040 features, 17.6% repeated from Fig. 2.

V. CONCLUSIONS

Computer vision methods for feature extraction, such as SIFT feature detector and Harris corner detector, are designed for images with rich texture and unsuitable to be used in retinal images. Repeatability of feature points in corresponding images is low and barely hitting beyond the 10% line for all approaches, especially when the viewing angle differences are large. Geometric corners which are on the bends and intersections between the blood vessels seem to be more stable and producing higher repeatability in the corresponding images. This is due to the observation that the blood vessels do not change that much in the retinal images. Future work will look into ways of describing these geometric corners into compact descriptors suitable for robust matching and mosaicing.

ACKNOWLEDGMENT

The authors would like to acknowledge the generous help from the National Healthcare Group, Eye Institute, Tan Tock Seng Hospital, Singapore. They provided the authors the clinical data with anonymity of patient information.

REFERENCES

[1] H. Bay, T. Tuytelaars and L. V. Gool. SURF: Speeded Up Robust Features. in Proc. European Conf. Computer Vision (ECCV), 2006, pp. 404–417.
[2] L. G. Brown. A survey of image registration techniques, ACM Comput. Survey. vol. 24, no. 4, 1992, pp. 325–376.
[3] M. Brown and D. G. Lowe. Recognising panoramas. in Proc. Int'l Conf. Computer Vision (ICCV), vol. 2, 2003, pp. 1218–1225.
[4] M. Brown, R. Szeliski and S. Winder. Multi-image matching using multi-scale oriented patches. in Proc. Int'l Conf. Computer Vision and Pattern Recog. (CVPR), vol. 1, 2005, pp. 510–517.
[5] P. C. Cattin, H. Bay, L. V. Gool and Székely, Gábor. Retina Mosaicing Using Local Features. in Proc. Int'l Conf. on Medical Image Computing and Computer-Assisted Intervention (MICCAI), vol. 3, 2006, pp. 185–192.
[6] J. Chen, J. Tian, N. Lee, J. Zheng, R. T. Smith and A. F. Laine. A Partial intensity invariant feature descriptor for multimodal retinal image registration. IEEE Trans. Biomedical Eng., vol. 57, no. 7, 2010, pp. 1707–1718.
[7] M. A. Fischler and R. C. Bolles. Random sample consensus: a paradigm for model fitting with applications to image analysis and automated cartography. in Proc. European Conf. Computer Vision (ECCV), 1996, pp. 683–695.
[8] C. Harris and M. Stephens. A combined corner and edge detector. in Proc. Alvey Vision Conf., 1988, pp. 147–151.
[9] H. Lester and S. Arridge. A survey of hierarchical nonlinear medical image registration. Pattern Recog., vol. 32, no. 1, 1999, pp. 129–149.
[10] D. G. Lowe. Distinctive image features from scale-invariant keypoints. in Int'l Journal of Computer Vision (IJCV), vol. 60, no. 2, 2004, pp. 91–110.
[11] M. K. Leung and Y. H. Yang. Dynamic two-strip algorithm in curve fitting. Pattern Recognition, vol. 23, no. 1-2, 1990, pp. 69–79.
[12] J. B. A Maintz and M. A. Viergever. A survey of medical image registration. Med. Image Anal., vol. 2, no. 1, 1998, pp. 1–36.
[13] V. S. Nalwa. Line-drawing interpretation: Straight lines and conic sections. IEEE Trans. Pattern Anal. and Machine Intelligence (TPAMI), vol. 10, no. 4, 1988, pp. 514–529.
[14] J. Shi and C. Tomasi. Good Features to Track. IEEE Conf. Computer Vision and Pattern Recog. (CVPR), 1994, pp. 593–600.
[15] E. Rosten and T. Drummond. Machine learning for high-speed corner detection. in Proc. European Conf. Computer Vision (ECCV), vol. 1, 2006, pp. 430–443.